INVESTIGATION OF CdZnS BUFFER LAYERS ON THE PERFORMANCE OF $CuInGaSe_2$ AND $CuGaSe_2$ SOLAR CELLS

Jiyon Song[1], Sheng S. Li[1], L. Chen[3], R. Noufi[4], T. J. Anderson[2], and O. D. Crisalle[2]
[1]Department of Electrical and Computer Engineering,
[2]Department of Chemical Engineering,
University of Florida, Gainesville, FL 32611, USA
[3]Energy Photovoltaics, Inc. (EPV), Lawrenceville, NJ 08648, USA
[4]National Renewable Energy Laboratory (NREL), Golden, CO 80401, USA

ABSTRACT

$Cu(In,Ga)Se_2$ (CIGS) and $CuGaSe_2$ (CGS) solar cells were fabricated using $Cd_{1-x}Zn_xS$ (CdZnS) buffer layers prepared by chemical bath deposition (CBD) with relative Zn compositions in the CBD bath values of x_{bath} = 0 (*i.e.,* pure CdS), 0.1, 0.2, 0.3, 0.4, and 0.5. The cell performance parameters of CIGS and CGS films treated with a KCN solution were investigated and compared to cells without KCN treatment. It was found that absorber films treated with KCN etching prior to the buffer CBD step show an improved cell performance for both the CIGS and CGS cells deposited with either CdS or CdZnS buffer layer. A CIGS cell with CdZnS buffer layer of x_{bath} = 0.2 produced a 13% AM1.5G conversion efficiency with higher V_{oc}, J_{sc}, and FF values as compared to the CdZnS/CIGS cells with different Zn contents. Results of photo- J-V and quantum efficiency (QE) measurements reveal that the CGS cell with CdZnS buffer layer of x_{bath} = 0.3 performed better than the CGS cell deposited with a pure CdS buffer layer. This result is suggested as a result of an increased photocurrent at shorter wavelengths and a more favorable conduction band-offset at the CdZnS/CGS junction.

INTRODUCTION

Fabricating a good $CuIn_{1-x}Ga_xSe_2$ (CIGS) p-n junction solar cell requires selecting an n-type buffer layer material with a lattice parameter that is well matched to the absorber layer as well has having favorable band offsets. The CdZnS ternary material with wurtzite structure gives the best lattice-match to the CIGS films over the entire range of x = [Ga] / ([Ga] + [In]) ratio, which leads to improved device performance in CIGS solar cells. The performance of cells with the wider band-gap CGS absorber material is inferior to the CIGS cells [1]. Based on the reported experimental studies, the most obvious limiting performance characteristic of CGS cells is the low open-circuit voltage (V_{oc}). For smaller band-gap CIGS absorbers with $E_g \leq 1.2$ eV and Ga content of $\approx$ 25-30 mol%, the value of V_{oc} increases at the same rate as the band-gap energy of CIGS absorbers. For wider band-gap CIGS absorbers (*i.e.*, $E_g \geq 1.2$ eV), the value of V_{oc} does not increase at the same rate as E_g, and hence device efficiency is reduced with increasing E_g. As-deposited p-type $CuInSe_2$ (CIS) films show an n-type In-rich inversion layer at the surface [2], while CGS films do not show the same surface inversion. For CIGS-based cells with CdS buffer layers, increasing the Ga content changes the conduction band offset at the heterojunction interface from a small spike for the CIS cells to a cliff for the CGS cells. The absence of an inverted surface layer in CGS cells and the barrier change at the heterojunction increase junction related recombination rates, which lead to a decrease in cell efficiency. Furthermore, the lattice-match between the CdS buffer and the CGS absorber is poor. Therefore, studies of alternative buffer layers for CGS cells are necessary.

Adding Zn to CdS buffer layer material decreases the lattice constant, which yields a better lattice-match to both CIGS and CGS absorber layers. The common-anion rule suggests that the valence band offset between two semiconductors having the same anion will be small, and this rule is supported by calculations for CdS/ZnS [5]. Increasing Zn composition in $Cd_{1-x}Zn_xS$ buffer films increases the band-gap energy (*i.e.*, CdS: x = 0, $E_g \approx 2.4$ eV, ZnS: x = 1, $E_g \approx 3.8$ eV), which results in a favorable conduction band offset with CIGS and CGS and an increase of the blue region response in CIGS and CGS cells. Therefore, CdZnS should lead to an increase of quantum efficiency (QE) in the shorter wavelength regime and a favorable conduction band-offset at the CdZnS and CIGS or CGS interface. It has been shown that adding Zn in CdS buffer layer enhances both the open-circuit voltage (V_{oc}) and short-circuit current density (J_{sc}), and hence a higher conversion efficiency for CGS solar cells [3]. In this paper, both CIGS and CGS cells with CdZnS buffer layers of different Zn compositions were fabricated to study the effects of adding Zn on the device performance.

DEVICE FABRICATION

In this work, all CIGS and CGS absorber films were provided by EPV and NREL, respectively. Prior to the deposition of the CdZnS buffer layers, an absorber film was etched in a 10 wt% KCN solution for four min to eliminate $Cu_{2-x}Se$ at the film surface. A buffer layer was then deposited by chemical bath deposition (CBD). The CBD reagents consisted of aqueous solutions of 1.20×10^{-3} M $CdCl_2\cdot2(1/2)H_2O$, 1.39×10^{-3} M NH_4Cl, 1.19×10^{-2} M thiourea (H_2NCSNH_2), 6.27×10^{-4} M $ZnCl_2$, and 5.27×10^{-4} M NH_3. By varying the relative ratio of Cd and Zn concentrations in the CBD bath, $Cd_{1-x}Zn_xS$ buffer films with Zn compositions of

x_{bath} = 0 (*i.e.*, pure CdS), 0.1, 0.2, 0.3, 0.4, and 0.5 were deposited on the CIGS and CGS absorber layers, where x_{bath} is denoted as the ratio of [Zn] / ([Zn] + [Cd]) in the CBD bath. In this paper, we have assumed that $x_{bath} = x$ (*i.e.*, x is the Zn alloy composition in CdZnS) for simplicity. The temperature in the CBD bath was maintained at ~85 °C during film deposition. The i-ZnO and n^+-ZnO bilayer films were then sputter-deposited by EPV. Ni/Al grid fingers with thicknesses of 50 nm/300 nm for the front contacts were deposited by electron-beam evaporation to obtain the finished cells. No antireflective coatings were applied to these cells. Finally, the cells were separated with isolation of each test cell by mechanical scribing. The total area of each test cell is 0.429 cm^2. The photocurrent density-voltage (photo- J-V) and quantum efficiency (QE) characteristics under AM1.5G (*i.e.*, 100 mW/cm^2 irradiance) and device temperature of 25.0±1 °C were measured in these cells.

DEVICE PERFORMANCE OF CdZnS/CIGS CELLS

Effects of KCN treatment on the performance of CIGS cells with CdS and CdZnS buffer layers

Table 1 summarizes the performance parameters of CdS/CIGS cells with and without KCN treatments. The CdS buffer layers were deposited by using the baseline CBD process with deposition times of 30 and 40 min. As shown in Table 1, the CIGS cells with KCN treatment were found to improve values of V_{oc}, J_{sc}, and FF, improving the device performance. Furthermore, the QE curve of the CdS/CIGS cells utilizing KCN treatment is higher than that of the cells without KCN treatment, as shown in Fig. 1. It was also observed that CdZnS/CIGS cells with KCN treatment improve overall device performance.

Table 1. Performance parameters of CdS/CIGS cells with and without KCN treatments on the CIGS absorber layer.

KCN	Deposition time (min)	V_{oc} (mV)	J_{sc} (mA/cm^2)	FF (%)	η (%)
(A) No	30	420	28.04	51.47	6.06
(B) Yes	30	482	31.22	65.10	9.80
(C) Yes	40	487	32.82	59.45	9.51

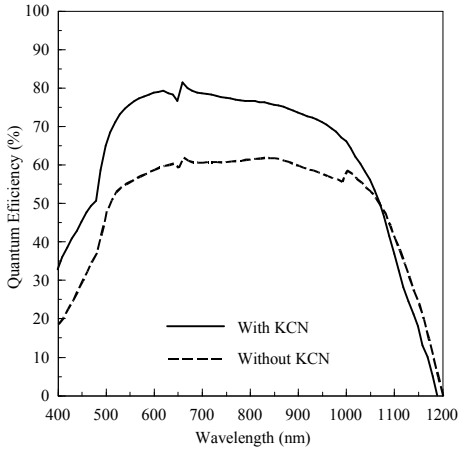

Fig. 1. QE of the CdS/CIGS cells shown in Table 1 (A and B).

Effects of CdZnS buffer layer thickness on the cell performance

The effect of CdZnS buffer layer thickness on the performance of CdZnS/CIGS cells can be assessed from the result presented in Table 2, which show the performance parameters of cells with relative Zn composition of x_{bath} = 0.3 and CBD deposition times of 40, 50, and 60 min. The buffer layer deposition times were increased from 40 to 60 min. FF was found to increase when the deposition time reached 60 min. The tested CdZnS/CIGS cells achieved higher J_{sc} as compared to those of the CdS/CIGS cells listed in Table 1, while at the same time realizing similar or slightly higher V_{oc}.

Table 2. Performance parameters of CdZnS/CIGS (x_{bath} = 0.3) cells with different CdZnS buffer layer deposition time.

Deposition time (min)	V_{oc} (mV)	J_{sc} (mA/cm^2)	FF (%)	η (%)
40	493	35.16	60.98	10.57
50	487	34.56	60.06	10.11
60	501	34.89	66.81	11.67

Note: All CIGS absorber films were treated by KCN.

Effects of Zn content in CdZnS buffer layers on the cell performance

A higher band-gap CdZnS buffer films can be obtained by increasing the relative Zn/Cd ratio in the CBD bath. A higher J_{sc} for the CdZnS/CIGS cell than that of CdS/CIGS cell is expected because of the higher QE in the shorter wavelength regime. Table 3 shows the dependence of device performance parameters on the Zn content in the CBD bath for CdZnS buffer layers with x_{bath} = 0 (CdS), 0.1, 0.2, 0.3, 0.4, and 0.5. The CdZnS/CIGS cell with x_{bath} = 0.2 achieved an AM1.5G conversion efficiency of around 13%, showing improved V_{oc}, J_{sc}, and FF among the CdZnS/CIGS cells with different x_{bath}. Furthermore, V_{oc} for the cell with x_{bath} = 0.2 increases by 44 mV compared to the CdS/CIGS cell, while J_{sc} increases about 4.38 mA/cm^2. Also note that starting with the composition x_{bath} = 0 (corresponding to a CdS/CIGS cell) the efficiency increases with increasing relative Zn content in the CdZnS/CIGS cell up to the composition x_{bath} = 0.2. The data show a decrease in efficiency for compositions with x_{bath} = 0.3 and 0.4, and a drastic reduction of efficiency for the Zn-rich CdZnS/CIGS cell with x_{bath} = 0.5. Fig. 2 shows the photo- J-V characteristics of CdZnS/CIGS cells for the same CIGS cells listed in Table 3. In addition to the results described above, a smaller buffer thickness with x_{bath} = 0.2 (see Table 3) gave a dramatic increase in cell efficiency compared to those for cells with x_{bath} = 0.3 and 0.4.

A direct comparison of QE for three of the cells (A, C, and F) shown in Fig. 2 is displayed in Fig. 3. As expected the QE of the cell incorporating a CdZnS buffer layer with a higher Zn content (x_{bath} = 0.5) is higher than that of the cell with a CdS and a lower Zn content (x_{bath} = 0.2) at shorter wavelengths because CdZnS is a wider band-gap material than CdS. This results in an increased value of J_{sc} as shown in Table 3 and Fig. 2. The QE of the CdZnS/CIGS cell with x_{bath} = 0.5 in the longer wavelength region, however, was found to be lower than that of the cell with x_{bath} = 0.2. This results in a slightly decreased J_{sc} of the CdZnS/CIGS cell with x_{bath} = 0.5 compared to that of the cell with x_{bath} =

0.2 as shown in Table 3. As mentioned above, using CdZnS buffer layers with wider band-gap values than CdS has a potential of increasing photocurrent generation particularly in the spectral region for wavelengths < 550 nm. The small difference in cut-off wavelength can be attributed to the difference in Ga content in the CIGS absorber layers. Further studies and optimization of the CdZnS buffer layer thickness and deposition conditions to improve the film quality are needed to better understand this buffer layer and achieving the highest performance possible.

Table 3. Performance parameters of CdZnS/CIGS cells as a function of Zn content in the CdZnS buffer layer.

x	Buffer layer thickness (nm)	V_{oc} (mV)	J_{sc} (mA/cm^2)	FF (%)	η (%)
(A) 0	40 ~ 50	482	31.22	65.10	9.80
(B) 0.1	60 ~ 70	517	32.85	66.31	11.25
(C) 0.2	~ 40	526	35.60	69.53	13.02
(D) 0.3	60 ~ 70	501	34.89	66.81	11.67
(E) 0.4	60 ~ 70	515	34.74	66.85	11.97
(F) 0.5	60 ~ 70	494	35.17	59.68	10.36

Note: All CIGS absorber films were treated by KCN.

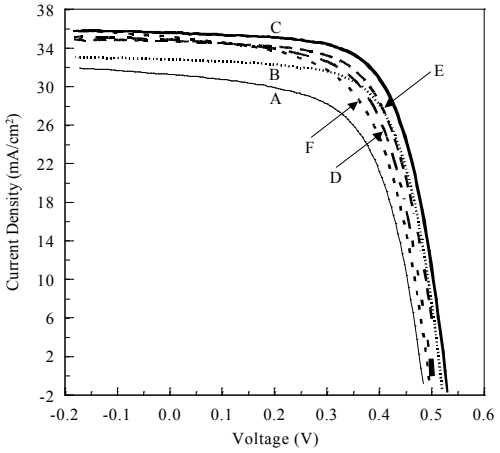

Fig. 2. Photo- J-V of CIGS cells shown in Table 3; (A) CdS, (B) x_{bath} = 0.1, (C) 0.2, (D) 0.3, (E) 0.4, and (F) 0.5.

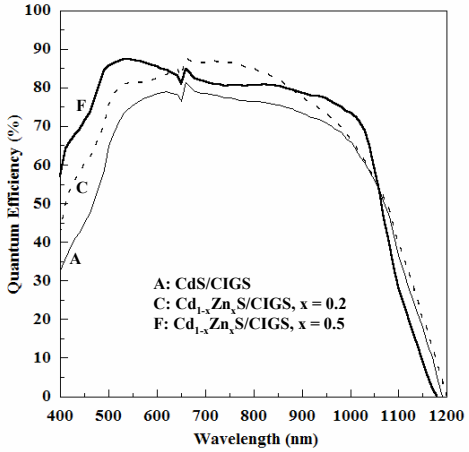

Fig. 3. A comparison of QE between (A) CdS/CIGS and CdZnS/CIGS cells; (C) x_{bath} = 0.2 and (F) 0.5.

DEVICE PERFORMANCE OF CdZnS/CGS CELLS

Effects of KCN treatment on the performance of CGS cells with CdS and CdZnS buffer layers

Based on studies of the characteristics of photo- J-V and QE of CIGS cells depicted above, it is suggested that a Zn content of x_{bath} = 0.2 to 0.3 is the optimal Zn content for the cell performance. A reduction in efficiency was found at a Zn content of x_{bath} = 0.5 or higher. Therefore, the CdZnS buffer layer with a Zn content of x_{bath} = 0.3 was used for fabricating CGS cells used in this study. Both CdS and CdZnS with x_{bath} = 0.3 buffer layers were deposited on the CGS samples. Table 4 shows the performance parameters of CdS/CGS and CdZnS/CGS cells with and without KCN treatments. The KCN treated CGS cells have improved V_{oc} and FF, resulting in better efficiency. The value of J_{sc} increased for the CdZnS/CGS cells with KCN treatment, while the value of J_{sc} for the CdS/CGS cell showed no improvement.

Table 4. Performance parameters of CdS/CGS and CdZnS/CGS (x_{bath} = 0.3) cells with and without KCN treatment of the CGS absorber layer.

KCN	*x*	V_{oc} (mV)	J_{sc} (mA/cm^2)	FF (%)	η (%)
No	0	352	15.05	41.87	2.22
Yes	**0**	**533**	**14.91**	**53.47**	**4.25**
No	0.3	394	12.22	35.96	1.73
Yes	**0.3**	**613**	**15.34**	**56.70**	**5.33**

Photo- J-V and QE characteristics of CGS cells with CdS and CdZnS buffer layers

Fig. 4 illustrates the photo- J-V characteristics of the CdS/CGS and CdZnS/CGS cells with KCN treatment listed in Table 4. As shown in Table 4 and Fig. 4, the V_{oc} of the CdZnS/CGS cell increases by 80 mV compared to that of CdS/CGS cell, while J_{sc} increases by 0.43 mA/cm^2. In fact, the CdZnS buffer layer provides a better conduction band offset with the CGS absorber layer than CdS [4]. As shown in Fig. 4, it is clearly demonstrated that CdZnS buffer layer improves V_{oc}, which is attributed to the reduced conduction band discontinuity at the junction. Furthermore, the replacement of CdS by CdZnS decreases window layer absorption losses, and hence increases values of J_{sc} and V_{oc} in the CGS cells. Fig. 5 shows the QE curves of the CdS/CGS and CdZnS/CGS cells shown in Fig. 4. It is clearly evident that the CdZnS/CGS cell has increased photocurrent generation at shorter wavelength (λ < 500 nm), resulting in a higher J_{sc} due to higher QE values. The CdS cell has slightly better collection in the longer wavelengths region. Therefore, the net current increase of the CdZnS cell is only ~0.43 mA/cm^2, as shown in Table 4. It was also observed that QE value for λ > 500 nm is limited to a maximum around 70%, which is presumably a consequence of losses in the collection of the photo-generated carriers. This could be due to a high recombination velocity and low diffusion length in the near surface region.

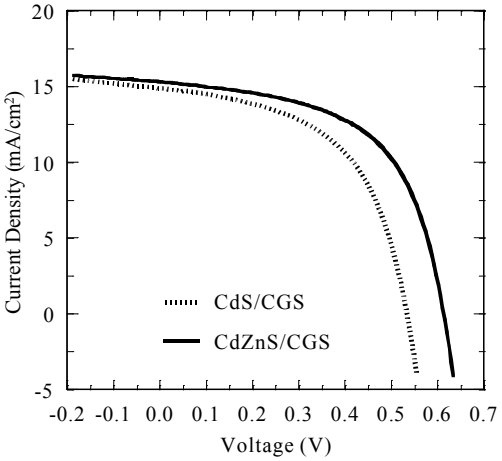

Fig. 4. Photo- J-V curves of CdS/CGS and CdZnS/CGS (x_{bath} = 0.3) cells shown in Table 4.

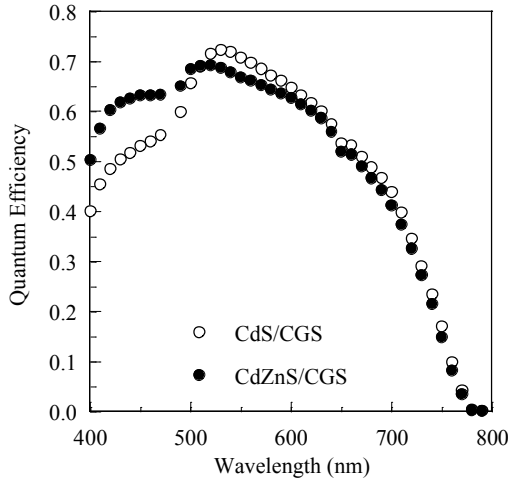

Fig. 5. QE curves of CdS/CGS and CdZnS/CGS (x_{bath} = 0.3) cells shown in Fig. 4.

SUMMARY AND CONCLUSIONS

Both CIGS and CGS solar cells deposited with CdS and CdZnS buffer layers have shown improvement in overall cell performance with KCN surface treatment compared to cells without KCN treatment. Adding Zn in CdS films results in improving the performance of CdZnS/CIGS cells as compared to that of CdS/CIGS cell. In particular, a CdZnS/CIGS cell with relative Zn composition of x_{bath} = 0.2 achieved a conversion efficiency of approximately 13% under AM1.5G conditions, showing improved V_{oc}, J_{sc}, and FF values compared to the CdS/CIGS cell and CdZnS/CIGS cells with different Zn contents. The 13% efficiency realized by using x_{bath} = 0.2 in the CdZnS/CIGS cell represents a 30% increase in efficiency over the reference CdS/CIGS cell used in this study. Furthermore, the wider band-gap CdZnS buffer layer increases the quantum efficiency of CdZnS/CIGS cells up to x_{bath} = 0.5 at shorter wavelengths as compared to that of CdS/CIGS cells. The CdZnS/CGS cell with Zn content of x_{bath} = 0.3 produced a conversion efficiency that is 25% higher than that of a CdS/CGS cell. Furthermore, values of V_{oc} for the CdZnS/CGS cell have increased by 80 mV as compared to that of a CGS cell deposited with a CdS buffer layer due to a reduced conduction band discontinuity at the CdZnS/CGS junction. It is also shown that the photocurrent generation in the shorter wavelengths (λ < 500 nm) of a CdZnS/CGS cell increased compared to the CdS/CGS cell.

ACKNOWLEDGEMENTS

This work was supported by the NREL High-Performance Photovoltaics Program under subcontract no. XAT-4-33624-15. The authors would like to acknowledge the support by EPV and NREL for providing CIGS and CGS absorber films used in this work.

REFERENCES

[1] J. AbuShama, R. Noufi, S. Johnston, S. Ward, and X. Wu, "Improved Performance in $CuInSe_2$ and Surface-Modified $CuGaSe_2$ Solar Cells", *31st IEEE PVSC*, 2005, pp. 299-302.

[2] D. Schmid, M. Ruckh, F. Grunwald, and H.W. Schock, "Chalcopyrite/Defect Chalcopyrite Heterojunctions on the Basis of $CuInSe_2$", *J. Appl. Phys*. **73**, No. 6, 1993, pp. 2902-2909.

[3] K.T. Ramakrishna Reddy, H. Gopalaswamy, and P. Jayarama Reddy, "Polycrystalline $CuGaSe_2$ Thin Film Solar Cells", *Vacuum*, **43**, No. 8, 1992, pp. 811-815.

[4] K.T. Ramakrishna Reddy and P. Jayarama Reddy, "Studies of $Zn_xCd_{1-x}S$ Films and $Zn_xCd_{1-x}S/CuGaSe_2$ Heterojunction Solar Cells", *J. Phys. D: Appl. Phys.* **25**, No. 9, 1992, pp. 1345-1348.

[5] S.-H. Wei and Alex Zunger, "Calculated Natural Band Offsets of All II-VI and III-V Semiconductors: Chemical Trends and the Role of Cation d Orbitals", *Appl. Phys. Lett.* **72**, 1998, pp. 2011-2013.